

Rockmagnetism and palaeomagnetism of an Early Cretaceous/Late Jurassic dike swarm in Rio Grande do Norte, Brazil

C. Bucker¹, A. Schult¹, W. Bloch², and S.D.C. Guerreiro³

¹ Institut für Allgemeine und Angewandte Geophysik, Theresienstraße 41/IV, D-8000 München 2, Federal Republic of Germany

² Institut für Geologie und Mineralogie, Schloßgarten 5, D-8520 Erlangen, Federal Republic of Germany

³ Núcleo de Ciências Geofísicas e Geológicas/UFPA, Caixa Postal 1611, 66000-Belém-Pará, Brasil

Abstract. Ten sites from a dike swarm of early Cretaceous/Late Jurassic age in northeast Brazil (5.7°S, 36.6°W) yielded a pole at 80.6°N, 95°E with $A_{95} = 9.5^\circ$, $K = 26.7$ after AF cleaning. Rock-magnetic investigations and chemical analyses revealed titanomagnetites and maghemites, both with low titanium content showing ilmenite exsolution lamellae (oxidation class III). These are due to an internal high-temperature oxidation during cooling of the large dikes, followed by low-temperature oxidation and/or hydrothermal alterations. There is evidence that with low-temperature oxidation the Ti-to-Fe ratio increases, a finding that is consistent with previous studies. Hysteresis parameters and susceptibility versus temperature curves can be interpreted in terms of pseudosingle-domain behavior with a trend toward multidomain behavior in accordance with moderate-to-weak stability of the remanence.

Key words: Rock magnetism – Palaeomagnetism – Basaltic dikes – South America

Introduction

Palaeomagnetic investigations in northeastern Brazil on Mesozoic volcanic rocks have been carried out by Schult and Guerreiro (1979, 1980) and by Guerreiro and Schult (1986). Preliminary palaeomagnetic results of a dike swarm in Rio Grande do Norte were published by Guerreiro and Schult (1983). In this paper, improved palaeomagnetic data and the rock magnetism of that dike swarm are presented.

Geological setting

The east-west-striking tholeiitic dike swarm in Rio Grande do Norte, northeast Brazil, extends over a distance of about 200 km (Fig. 1). The individual dikes are 5–50 m wide. The swarm can be divided into three subswarms (I, II, and III).

Radiometric determinations on three samples (whole rock) with the K/Ar method (cited in Sial, 1976) and on three samples with the fission track method (Sial, 1974) yielded ages between 125 and 131 m.y. with a mean of 128 m.y. (Early Cretaceous). New potassium-argon determinations were performed on samples from four sites (Fig. 1). Whole-rock isochrones yielded the following ap-

parent ages: site 43: 161 m.y.; site 44: 145 m.y.; site 46: 130 m.y.; site 47: 137 and 167 m.y. All rocks investigated were weathered and therefore not very suitable for age dating. The reported ages are probably minimum ages (the measurement details will be published elsewhere). These new data indicate that the age is Late Jurassic rather than Early Cretaceous. In recent publications (e.g., Mapa Geológico do Brasil, 1981) Early Cretaceous has been the age assigned to the dikes.

In the vicinity of the dikes, Tertiary necks and flows are also found (Fig. 1). K/Ar determinations on three samples from three necks yielded an age of about 18 m.y. (cited in Sial 1976). The best known of these necks, the Pico do Cabugi, is situated east of Lages on a dike.

Palaeomagnetism

The site locations selected are shown in Fig. 1. Samples (2.5 cm in diameter and 2.3 cm length) were taken with a portable drill. Some of details regarding the palaeomagnetic measurements and preliminary results have been published elsewhere (Guerreiro and Schult, 1983). For several sites, the palaeomagnetic data could be improved by more rigorous AF cleaning. The vector diagrams in Fig. 2 show that in some cases relatively high fields are necessary to erase secondary components. Such high fields were not applied in the first instance. The final results are summarized in Table 1. From 14 sites selected, 10 were used for the overall mean: For three sites (48, 53 and 54), no consistent results could be achieved (it is possible that from site 54 rolled blocks were sampled), and site B3 was discarded because it is not a dike but a basalt flow (of Tertiary age).

After AF cleaning, the mean direction of the characteristic remanent magnetization (CARM) was $D = 186.6^\circ$, $I = +20.8^\circ$ with $N = 10$, $\alpha_{95} = 14.1^\circ$, $k = 12.6$ yielding a pole at 80.6°N, 95°E with $A_{95} = 9.5^\circ$, and $K = 26.7$. Seven sites had reversed polarity (all from dike I and II) and three sites normal polarity (all from dike III). These results supersede the previous findings (Guerreiro and Schult 1983). However, there is little difference between results.

Figure 3 compares the new pole position with Early Cretaceous and Jurassic poles from stable South America (for compilation, see Schult et al., 1981; Guerreiro and Schult, 1986). The new (Early Cretaceous or Late Jurassic) pole is nearer to the Jurassic poles and lies at the edge of the Early Cretaceous pole distribution.

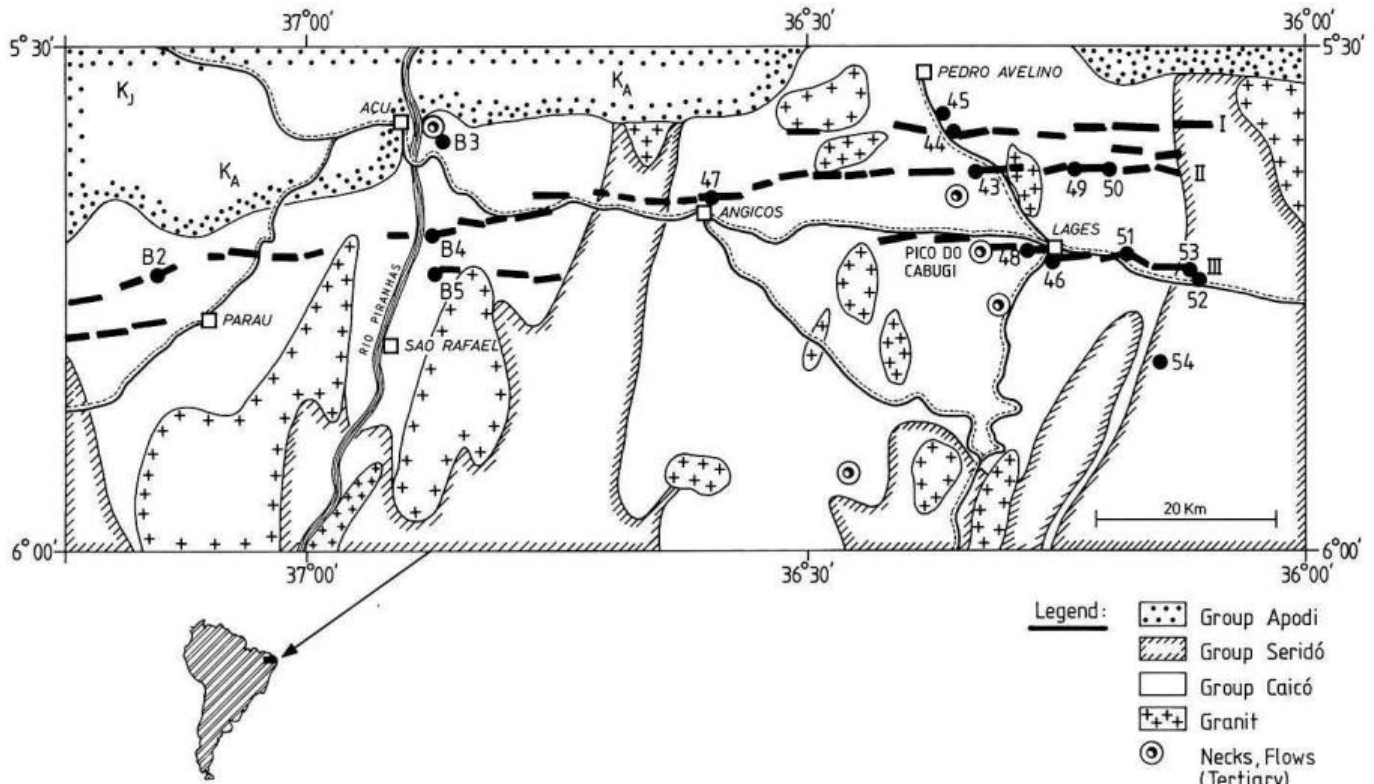


Fig. 1. Geological sketch map and sampling sites in Rio Grande do Norte, NE Brazil

Table 1. Palaeomagnetism of a dike swarm in Rio Grande do Norte (ca. 5.7°S, 36.6°W)

Site/dike	NRM						CARM					VGP	
	<i>N</i>	<i>D</i>	<i>I</i>	α_{95}	<i>k</i>	MDF (Oe)	<i>N</i>	<i>D</i>	<i>I</i>	α_{95}	<i>k</i>	°N	°E
43/II	9	231	+57.2	17.9	9	180	9	190.1	+51.6	3.9	174	61.8	125
44/I	11	196	-16.4	16.9	8	40	9	177.2	-5.3	2.6	387	81.2	305
46/III	10	357	-19.8	10.5	22	50	14	4.2	-3.3	4.1	91	84.2	10
47/II	7	223	+19.6	10.0	37	120	8	210.1	+33.5	4.2	169	58.0	79
48/III	15	No consistent results				50	15	No consistent results					
49/I	8	No consistent results				250	7	178.2	-2.3	6.1	97	82.9	309
50/II	5	304	+41.1	70	2	130	5	183.6	+38.6	15.8	25	73.6	132
51 a/III	8	No consistent results				60	8	No consistent results					
51 b/III	6	5	-10.5	19.0	13	180	8	1.9	-11.1	5.8	91	88.1	51
53/III		No consistent results				150		No consistent results					
54		No consistent results				50		No consistent results					
B2/II	5	204	+11.4	24.6	11	90	6	191.9	+40.1	3.2	436	69.4	110
B3	9	358	+17.4	30.8	9	240	9	(9.4	+18.0	5.2	97	72.4	355)
B4/II	4	227	+19.9	48.0	5	180	4	196.1	+34.5	8.3	125	69.5	95
B5/III	7	0	-5.5	3.5	239	130	7	0.9	-0.9	5.1	138	84.7	333
Mean of site means							10	186.6	+20.8	14.1	12.6	80.6	95.1
												$K=26.7$	$A_{95}=9.5$

N, number of samples; *D*, declination; *I*, inclination; α_{95} and A_{95} , radius of 95% confidence circle; *k* and *K*, precision parameter; MDF, medium destructive peak field necessary to erase half of NRM intensity by alternating field demagnetization; 1 Oe \approx 79.58 Am⁻¹

Rock magnetism

The methods used to identify the magnetic minerals in basaltic rocks were X-ray investigations, microscopic investigations, chemical analyses, and measurements of magnetic

properties such as Curie temperature and temperature dependence of high-field magnetization and of susceptibility. The temperature dependence of specific high-field magnetization J_s and Curie temperature T_c were determined by means of an automatically recording balance in a field of

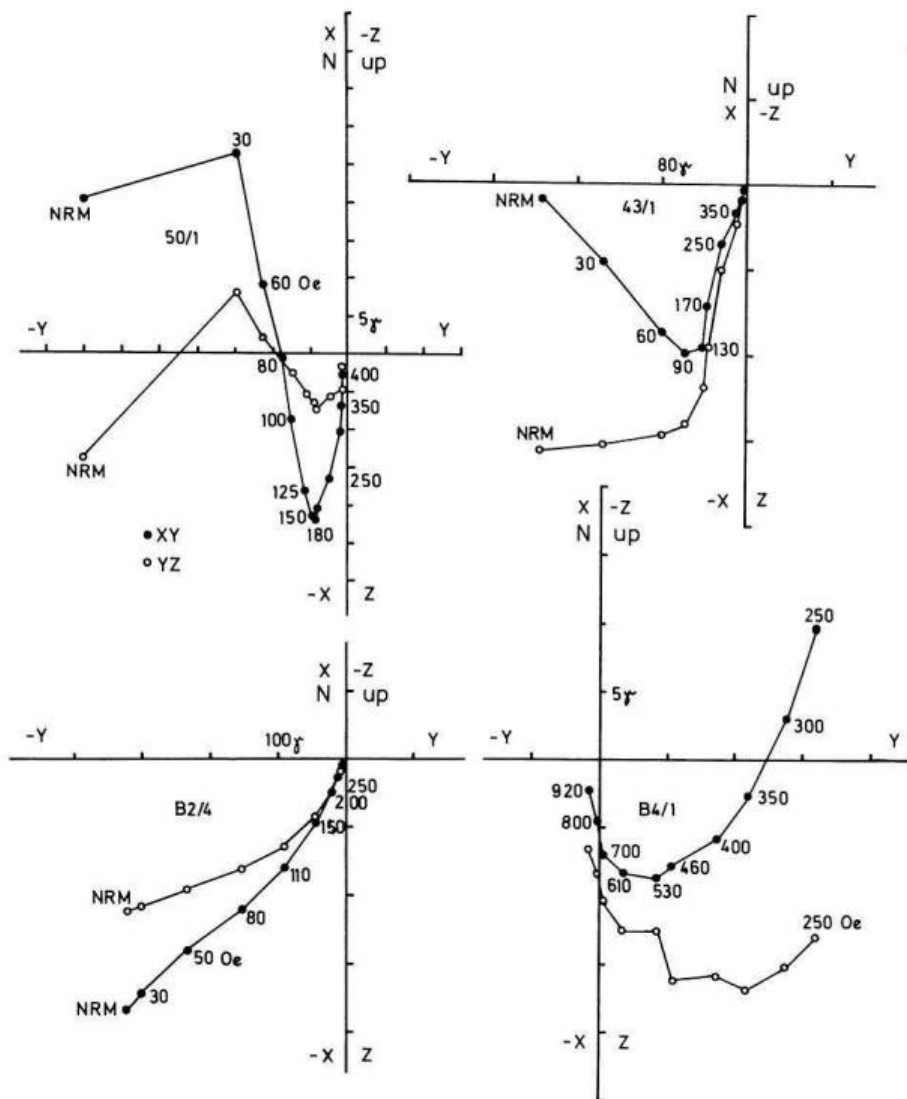


Fig. 2. Vector diagrams showing the variation of the remanence during progressive AF demagnetization. *Open* and *solid* symbols indicate components in the vertical EW and horizontal planes, respectively

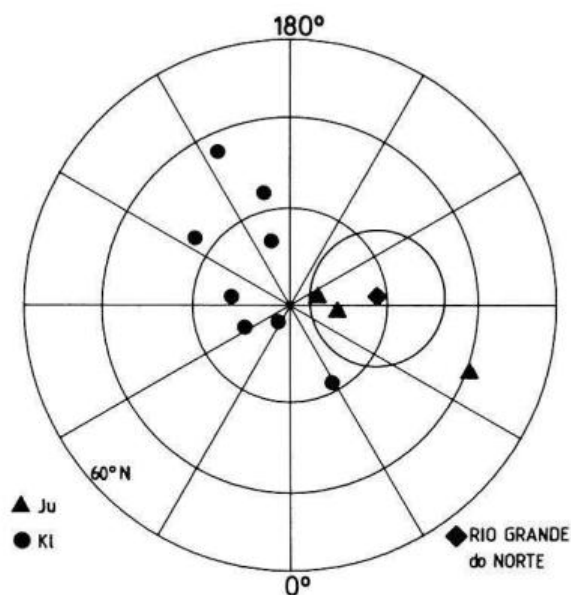


Fig. 3. Compilation of Early Cretaceous and Jurassic poles (this paper; Schult et al., 1981; Guerreiro and Schult, 1986)

about 1800 Oe ($1 \text{ Oe} = 79.58 \text{ Am}^{-1}$). The measurements were carried out in air on whole (moderately crushed) rock. Table 2 summarizes the results.

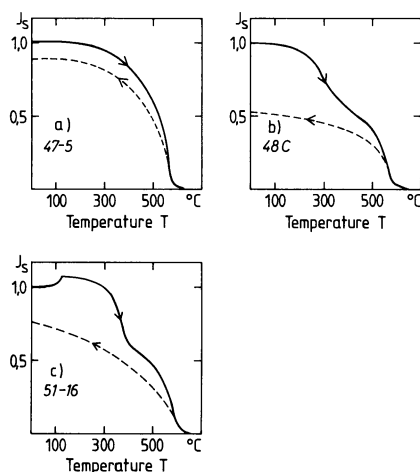
The typical $J_s(T)$ curves obtained are shown in Fig. 4; Fig. 4a indicates a composition near magnetite with low titanium content. The $J_s(T)$ curves of most samples are similar to Fig. 4b. This curve is symptomatic for the presence of some maghemite (with low titanium content), in addition to magnetite, and is characterized by the irreversible decrease of J_s between 350° and 480° C due to transformation of maghemite to hematite. The portion of (decomposing) maghemite was estimated from the irreversible decrease of J_s (see Table 2). Some samples showed a kink type $J_s(T)$ curve (Fig. 4c) (Ade-Hall et al., 1971). The kink (irreversible maximum near 150° C) was only observed in connection with maghemite decomposition at about 380° C . The shape of the kink depends on field strength: with decreasing field strength, the kink becomes more pronounced, which implies the presence of a magnetic phase with relative high coercivity that decreases strongly with increasing temperature.

For X-ray investigations, the samples were pulverised and the magnetic phase separated with a hand magnet. In

Table 2. Rockmagnetic data

Sample	a (Å)	T_c (°C)	J_s	T_{ph} (°C)	Other phases	x	z
B 2/3	(8.399)	550	b, Mt, Mgh (15%)		Ilm	0.11	0.25
B 3/7	8.395	575	a, Mt	+	Ilm, Hm	0.03	0.15
B 4/5	8.403	560	b, Mt, Mgh (15%)	+	Ilm	0.07	0.1
B 5/3	8.386	565	b, Mt, Mgh (15%)		Ilm	0.1	0.45
43/10	8.371	575	c, Mt, Mgh (35%), k		Ilm	0.15	0.75
44/3	8.399	560	a, Mt	+	Ilm, Hm	0.08	0.17
46/2	8.400	570	a, Mt	-150	Ilm	0.04	0.1
47/5	8.395	570	a, Mt	-165	Ilm	0.02	0.15
48/3	8.400	575	b, Mt, Mgh (20%)	-145	Ilm, Hm	0	0
48/F2	8.396	575	b, Mt, Mgh (25%)	-155	Ilm	0.03	0.2
49/2	8.387	575	b, Mt, Mgh (5%)		Ilm	0.08	0.5
50/4	8.354	570	c, Mt, Mgh (70%)		Ilm	0.26	0.9
51 a/3	8.403	580	a, Mt	-175	Ilm	0	0
51 b/16	(8.385)	580	c, Mt, Mgh (40%), k		Ilm, Hm	0.06	0.5
53/1	8.400	570	b, Mt, Mgh (20%)	-165	Ilm, Hm	0.05	0.1
54/4	8.398	575	b, Mt, Mgh (20%)	-155	Ilm, Hm	0.03	0.1

a , Lattice constant, error about 0.003 Å (in parentheses >0.003 Å); T_c Curie temperature; $J_s(T)$ curves are shown in Fig. 4; Mt, magnetite; Mgh, maghemite; parentheses, portion of maghemite estimated from irreversible decrease of J_s between 350° and 480° C; k , kink type $J_s(T)$ curve (Ade-Hall et al., 1971); T_{ph} low-temperature phase transition of magnetite according decrease of susceptibility (Fig. 6); +, transition indicated; other phases (detected by ore microscopy and X-ray investigation): Ilm, ilmenite; Hm, hematite; x , composition in $(1-x)\text{Fe}_3\text{O}_4 \times \text{Fe}_2\text{TiO}_4$ and z oxidation parameter estimated from T_c and a (after Readman and O'Reilly, 1972)

**Fig. 4.** Examples of thermomagnetic curves as described in the text

some cases, this procedure was repeated several times. A Debye-Scherrer camera with 114.83 mm diameter and cobalt radiation was used. The lattice constant of the titanomagnetites was determined and other iron titanium oxides were identified if sufficiently present. The titanium content x and the oxidation parameter z of the titanomagnetites derived from the lattice constants and the Curie temperatures (Readman and O'Reilly, 1972) are also listed in Table 2 and shown in Fig. 5.

For all samples, microscopic observations on polished sections showed ilmenite exsolution lamellae in magnetite grains that were consistent with the X-ray investigations. This finding can be classified with oxidation class III due to high-temperature oxidation according to Wilson and Watkins (1967). The occurrence of shrinkage gaps in the magnetite grains of several samples indicate low-temperature oxidation consistent with the presence of maghemite in the majority of samples.

The temperature dependence of the susceptibility was measured with a Highmoor susceptibility bridge between -196° and 700° C. Typical $\chi(T)$ curves are shown in Fig. 6. The Curie temperatures derived from these curves and also the presence of maghemite can be seen from the $\chi(T)$ curves. For magnetite, a decrease of susceptibility can be observed at about -150° C due to phase transition from cubic to orthorhombic and vanishing magnetocrystalline anisotropy constant K_1 . The transition temperature decreases with increasing titanium content (to about -220° C for $x=0.1$) (Collison et al., 1967). For several samples (Fig. 6 and Table 2), such a transition temperature (above -200° C) was detected, which indicated a relatively low titanium content that was qualitatively in agreement with the derived x values from the contour diagram or with the chemical analyses (see below).

The chemical analyses were carried out with a transmission electron microscope with energy dispersive equipment (Table 3). In all cases, a small amount of silicon was measured. As it is generally accepted that titanomagnetites and ilmenites contain practically no silicon, it is assumed that the silicon measured is due to contamination by adjacent silicates. The number of cations per formula unit was calculated, omitting silicon and assuming stoichiometry (see Table 3). In most cases, there was agreement between the titanium content obtained with the two methods (Tables 2 and 3), except for sample 50/4. This sample contained predominantly maghemite, which decomposed before its true Curie temperature was reached, yielding too low a Curie temperature and therefore too much titanium content in the contour diagram (Fig. 5). To a certain extent this was also valid for sample 43. The other metallic cations (Al, Mg, Mn, Cr, V) seemed to have relatively little influence on the contour diagram, so that the titanium content was essentially correct. At least for the lattice constant, some of these metallic cations have opposite effects: for magnetite it is increased by substitutions by Mn and V and decreased by Al, Mg, and Cr (Bleil and Petersen, 1982).

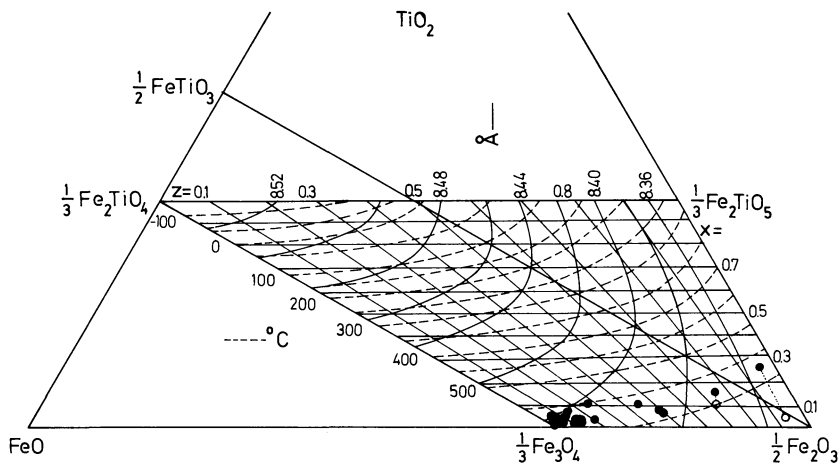


Fig. 5. Composition of titanomaghemites from the basaltic dike swarm using the contour diagram after Readman and O'Reilly (1972) and the Curie temperatures and lattice constants as listed in Table 2. The few open circles denote the deviating titanium content measured with a transmission electron microscope. Lines of equal oxidation parameter z are also given

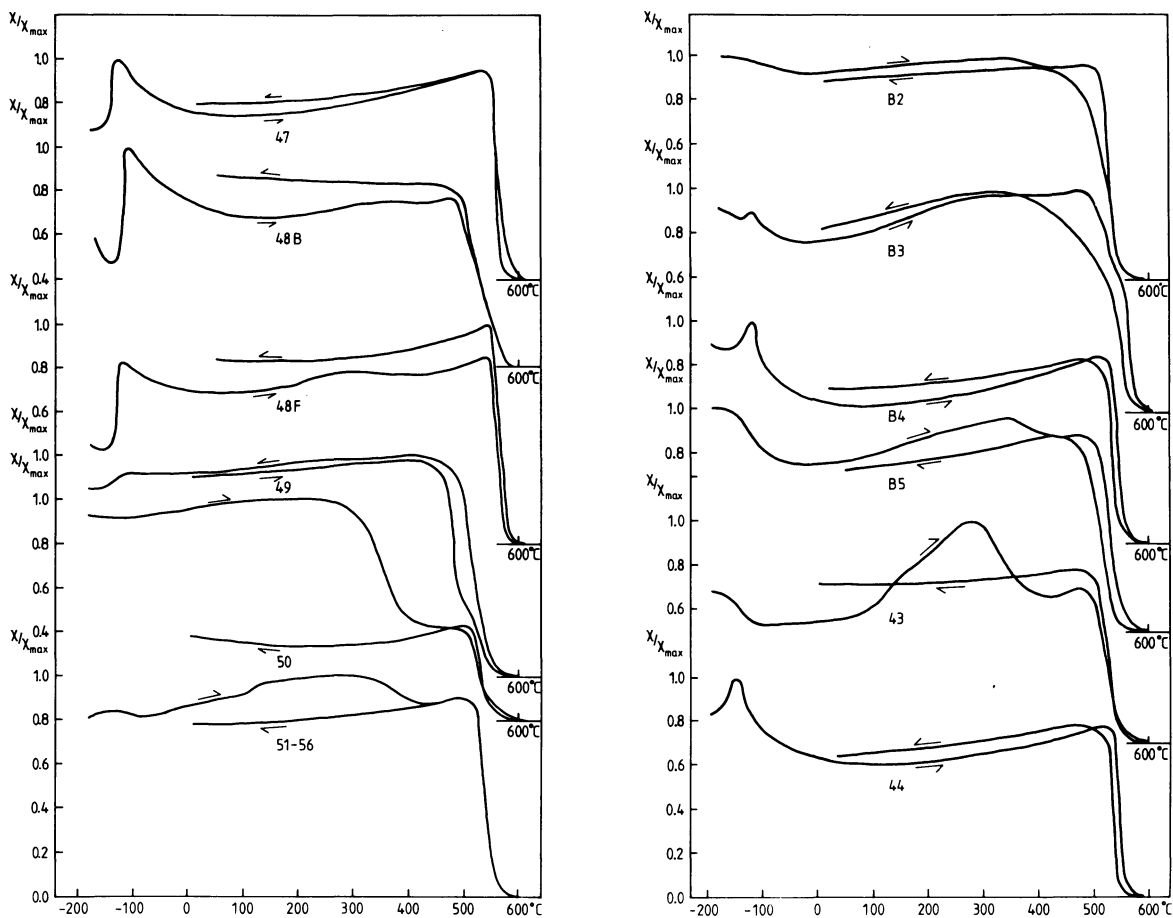


Fig. 6. Temperature dependence of susceptibility

The degree of the low-temperature oxidation of the titanomaghemites was generally not homogeneous. In several cases, the $J_s(T)$ curves indicated some amount of maghemite (i.e., z near unity) whereas the z value obtained from the contour diagram was small (e.g., samples B2, B4, 48, 53, 54). Despite this difficulty, it can be assumed that the z values represent mean values for the samples. Figure 5 is consistent with the finding in many studies that low-temperature oxidation of titanomagnetite involves the mi-

gration of iron away into the surrounding matrix, resulting in an increase in the Ti-to-Fe ratio of the remaining phase (e.g., Marshall and Cox, 1972; Petersen et al., 1979; Furuta et al., 1985). This behavior has been particularly supported by studies on basaltic rocks from the sea floor (titanomaghemites with x values of about 0.6). In our study, the titanomaghemites in the subaerial basaltic rocks had low x values (≈ 0.04) at the beginning of the low-temperature oxidation.

These (titano-) magnetites are probably the result of

Table 3. Chemical analyses of iron titanium oxides

Sample	<i>N</i>	Fe	Ti	Al	Mg	Mn	Cr	V	Si	Fe	Ti	Al	Mg	Mn	Cr	V	<i>x</i>
(atom percent)										(cations)							
B2																	
Tmt	15	93.4	3.6	0.7	—	0.3	0.7	—	0.6	2.84	0.11	0.02	—	0.01	0.02	—	0.11
Ilm	13	48.4	47.0	0.6	0.6	2.0	—	—	1.4	0.98	0.95	0.01	0.01	0.04	—	—	
B3																	
Tmt	12	95.9	1.7	0.7	0.3	0.7	—	—	0.7	2.90	0.05	0.02	0.01	0.02	—	—	0.03
Ilm	4	47.1	47.0	0.8	2.8	1.3	—	—	0.8	0.95	0.95	0.02	0.06	0.03	—	—	
B4																	
Tmt	10	94.5	2.3	0.6	0.4	0.4	—	1.1	0.6	2.85	0.07	0.02	0.01	0.01	—	0.03	0.07
Ilm	3	48.0	48.5	1.0	0.3	1.3	—	—	0.9	0.97	0.98	0.02	0.01	0.03	—	—	
Rt	2	3.7	93.5	1.2	0.2	0.2	—	—	1.1	0.04	0.95	0.01	0	0	—	—	
B5																	
Tmt	12	93.4	3.0	0.8	0.4	0.4	—	0.6	0.8	2.84	0.09	0.02	0.01	0.01	—	0.02	0.1
Ilm	3	48.8	46.4	0.9	1.3	1.4	—	—	1.2	0.99	0.94	0.02	0.03	0.03	—	—	
43/10																	
Tmt	11	92.1	3.5	1.0	0.3	0.4	—	1.2	1.5	2.81	0.11	0.03	0.01	0.01	—	0.03	0.15
Ilm	5	49.0	48.0	0.6	0.4	1.6	—	—	0.4	0.98	0.96	0.01	0.01	0.03	—	—	
Per	1	8.3	58.9	2.4	0.5	0.4	—Ca	27.4	2.8								
44																	
Tmt	9	93.9	1.9	1.5	0.5	—	—	—	1.2	2.88	0.06	0.05	0.02	—	—	—	0.08
Ilm	11	50.9	45.2	0.6	0.5	1.7	—	—	1.2	1.02	0.92	0.01	0.01	0.03	—	—	
Pyr	1	42.9	0.8	0.7	0.5	0.2	—S	52.3	2.0	0.95	0.02	0.02	0.01	0	—	S1.16	
46/2																	
Tmt	9	96.9	1.5	0.6	0.2	0.3	—	—	0.5	2.92	0.05	0.02	0.01	0.01	—	—	0.04
Ilm	3	47.7	48.0	0.7	—	2.8	—	—	0.7	0.96	0.97	0.01	—	0.06	—	—	
Rt	1	4.8	92.0	1.2	0.5	0.3	—	—	1.2	0.05	0.93	0.01	0.01	0	—	—	
47																	
Tmt	8	96.7	0.9	0.6	0.3	0.3	—	0.7	0.5	2.92	0.03	0.02	0.01	0.01	—	0.02	0.02
Ilm	3	48.2	48.0	1.0	—	1.4	—	—	1.3	0.98	0.97	0.02	—	0.03	—	—	
48/3																	
Tmt	7	96.0	0.7	0.6	0.8	0.1	—	—	1.6	2.93	0.02	0.02	0.02	0.01	—	—	0
Ilm	3	47.5	47.8	0.7	0.9	2.0	—	—	0.9	0.96	0.97	0.01	0.02	0.04	—	—	
48/F2																	
Tmt	8	97.0	1.0	0.6	0.3	0.1	—	—	1.0	2.94	0.03	0.02	0.01	0	—	—	0.03
Ilm	3	48.3	47.9	0.7	0.8	1.1	—	—	1.5	0.98	0.97	0.01	0.02	0.02	—	—	
49/2																	
Tmt	7	94.2	3.5	0.8	0.5	—	—	—	1.0	2.85	0.10	0.02	0.02	—	—	—	0.08
Ilm	3	48.2	47.9	0.7	0.7	1.4	—	—	1.0	0.97	0.97	0.01	0.01	0.03	—	—	
50/4																	
Tmt	10	97.2	1.3	0.5	0.2	0.3	—	—	0.5	2.93	0.04	0.02	0.01	0.01	—	—	(0.26)
Ilm	2	48.3	47.2	0.7	0.9	1.5	—	—	1.3	0.98	0.96	0.01	0.02	0.03	—	—	
51/16																	
Tmt	10	94.7	2.0	1.0	0.5	0.1	—	—	0.5	2.89	0.06	0.03	0.02	0	—	—	0.06
Ilm	9	51.5	43.0	0.8	0.7	1.7	—	—	1.5	1.05	0.88	0.02	0.01	0.03	—	—	
54/4																	
Tmt	7	95.8	1.8	0.5	—	—	—	1.3	0.5	2.89	0.05	0.02	—	—	—	0.04	0.03
Chr	4	47.5	1.0	0.3	—	—	50.0	0.6	0.8	1.43	0.03	0.01	—	—	1.51	0.02	

Analyses are given in atom percent (total 100%). Number of cations (per formula unit) was calculated assuming stoichiometry and omitting Si. *N*, number of analyses; *x* from Table 2, to compare with Ti or the sum of Ti and other metallic ions. Tmt, titanomagnetite; Ilm, ilmenite; Rt, rutile; Per, perovskite; Pyr, pyrrhotite; Chr, chromite

an “internal oxidation” during cooling of the (large) dikes, a special case of high-temperature oxidation. From the coexisting titanomagnetites and ilmenites, the temperature of their formation can be inferred (Buddington and Lindsley, 1964). The temperatures obtained are very low, ranging from 500° to 600° C. This would mean that the remanence

could be, in part, thermochemical remanent magnetization rather than thermal remanent magnetization. The low-temperature oxidation was evident for all samples. Also, hydrothermal alteration is possible. According to Ade-Hall et al. (1971), the kink type $J_s(T)$ curve is indicative for this alteration.

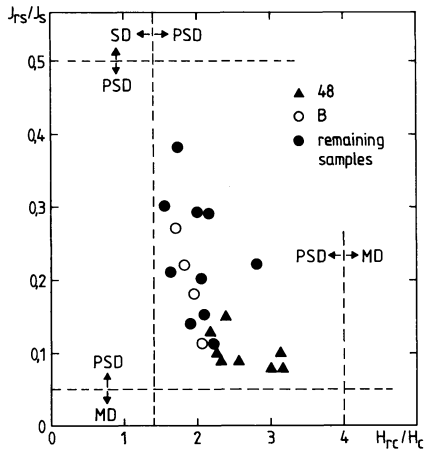


Fig. 7. J_{rs}/J_s versus H_{rc}/H_c . The horizontal and vertical lines indicate the single-domain (SD) pseudo single domain (PSD) transition and PSD multidomain (MD) transition, respectively (Day et al., 1977)

Hysteresis parameters

Relations between quotients H_{rc}/H_c (remanence coercivity, coercivity) and J_{rs}/J_s (saturation remanence, saturation magnetization) can be used to distinguish between different domain structure types (Day et al., 1977). Figure 7 shows PSD behavior for all samples with a trend to MD behavior. The weak Hopkinson peaks of the $\chi(T)$ curves (Fig. 6) indicate PSD with a trend toward MD behavior of the oxide grains as well (Dunlop, 1974). According to the microscopic observations, the magnetite grains are relatively large (several micrometers) despite the subdivision of the oxide grains by ilmenite lamellae. This is also in accordance with weak stability of the remanence in several cases (Table 1).

Conclusions

1. The mean pole position for the Lower Cretaceous or Late Jurassic dike swarm in Rio Grande do Norte compares favorably with other poles of South America.
2. The ferrimagnetic minerals are magnetites and maghemites with a low titanium content and still less of other metallic cations, such as Al, Mg, Mn, Cr, and V.
3. The magnetites have been affected by high-temperature oxidation during cooling of the large dikes. The magnetites show ilmenite exsolution lamellae (oxidation class III). The geothermometer (Buddington and Lindsley 1964) yields low temperatures (500°–600° C).
4. The magnetites have undergone low-temperature oxidation of varying degrees. Of the samples 70% also contain maghemite. There are indications of hydrothermal alterations.
5. There is evidence that, with low-temperature oxidation, the Ti-to-Fe ratio increases, which is consistent with previous studies on basaltic rocks from the ocean floor.
6. Hysteresis parameters can be interpreted in terms of PSD behavior with a trend approaching MD behavior. The stability of the remanence is moderate and in some cases weak.
7. The titanium content determined with the aid of the contour diagram according to Readman and O'Reilly (1972) is in agreement with microprobe chemical analysis.

Acknowledgements. We thank Prof. Dr. R. Schwab for his advice and help in the field work and Dr. P. Horn and Dr. D. Müller-

Sohnius (Institut für Mineralogie und Petrologie, München) for the potassium-argon determinations. This research was done within the bilateral agreement between Brazil and the Federal Republic of Germany within the Geochemistry Project. The financial support of Bundesministerium für Forschung und Technologie, Conselho Nacional de Desenvolvimento Científico e Tecnológico and Deutsche Forschungsgemeinschaft is gratefully acknowledged.

References

- Ade-Hall, J.M., Palmer, H.C., Hubbard, T.P.: The magnetic and opaque petrological response of basalts to regional hydrothermal alteration. *Geophys. J.R. Astron. Soc.* **24**, 137–174, 1971
- Bleil, U., Petersen, N.: Magnetic properties of natural minerals. In: Landolt-Börnstein, New Series, Group V, Vol. 1b, G. Angenheister ed.: pp. 308–365. Heidelberg, New York: Springer 1982
- Buddington, A.F., Lindsley, D.H.: Iron-titanium oxide minerals and synthetic equivalents. *J. Petrol.* **5**, 310–357, 1964
- Collinson, D.W., Creer, D.M., Runcorn, S.K.: Methods in paleomagnetism. Amsterdam: Elsevier 1967
- Day, R., Fuller, M., Schmidt, V.A.: Hysteresis properties of titanomagnetites: grain-size and compositional dependence. *Phys. Earth Planet. Interiors* **13**, 260–267, 1977
- Dunlop, D.J.: Thermal enhancement of magnetic susceptibility. *J. Geophys.* **40**, 439–451, 1974
- Furuta, T., Otsuki, M., Akimoto, T.: Quantitative electron probe microanalysis of oxygen in titanomagnetites with implications for oxidation process. *J. Geophys. Res.* **90**, 3145–3150, 1985
- Guerreiro, S.D.C., Schult, A.: Palaeomagnetismo de um exame de diques toleíticos de idade meso-cenozoica, localizados no Rio Grande do Norte. *Rev. Bras. Geofis.* **1**, 89–98, 1983
- Guerreiro, S.D.C., Schult, A.: Palaeomagnetism of Jurassic tholeiitic intrusions in the Amazon Basin. Veröffentlichung des Geophysikalischen Observatoriums Fürstfeldbruck, Münchner Universitätsschriften, Serie B, Nr. 10, 61–72, 1986
- Mapa Geológico do Brasil, Ministério das Minas e Energia, DNPM, 1981
- Marshall, M., Cox, A.: Magnetic changes in pillow basalt due to sea floor weathering. *J. Geophys. Res.* **77**, 6459–6469, 1972
- Petersen, N., Eisenach, P., Bleil, U.: Low temperature alteration of the magnetic minerals in ocean floor basalts. In: Maurice Ewing Series 2, M. Talwani, C.G. Harrison, D.E. Hayes (eds.), pp. 169–209. Washington O.C.: American Geophysical Union 1979
- Readman, P.W., O'Reilly, W.: Magnetic properties of oxidized (cation-deficient) titanomagnetites (Fe, Ti)₃O₄. *J. Geomagn. Geoelectr.* **24**, 69–90, 1972
- Schult, A., Guerreiro, S.D.C.: Palaeomagnetism of Mesozoic igneous rocks from the Maranhao Basin, Brazil and the time of opening the South Atlantic. *Earth Planet. Sci. Lett.* **42**, 427–436, 1979
- Schult, A., Guerreiro, S.D.C.: Palaeomagnetism of Upper Cretaceous volcanic rocks from Cabo de Sto. Agostinho, Brazil. *Earth Planet. Sci. Lett.* **50**, 311–315, 1980
- Schult, A., Hussain, A.G., Soffel, H.C.: Palaeomagnetism of Upper Cretaceous volcanics and Nubian sandstones of Wadi Natash, SE Egypt and implications for the polar wander path for Africa in the Mesozoic. *J. Geophys.* **50**, 16–22, 1981
- Sial, A.N.: Petrology and tectonic significance of the post-Palaeozoic basaltic rocks of northeast Brazil. Ph.D. Thesis, University of Columbia, 403 pp., 1974
- Sial, A.N.: The post-Palaeozoic volcanism of northeast Brasil and its tectonic significance. *Ann. Acad. Bras. Cienc. [Suppl]*, **48**, 299–311, 1976
- Wilson, R.W., Watkins, N.D.: Correlation of petrology and natural magnetic polarity in Columbia Plateau basalts. *Geophys. J.R. Astron. Soc.* **12**, 405–424, 1967

Received April 21, 1986; revised version August 15, 1986
Accepted August 22, 1986